Folding and Unfolding of Individual PNIPAM-*g*-PEO Copolymer Chains in Dilute Aqueous Solutions

Hongwei Chen,[†,‡] Junfang Li,[†] Yanwei Ding,[‡] Guangzhao Zhang,[†] Qijin Zhang,[*,‡] and Chi Wu[*,†,§]

Structure Research Laboratory, Department of Polymer Science and Engineering, University of Science and Technology of China, Hefei, Anhui, China; Laboratory of Macromolecular Colloids and Solutions, The Hefei National Laboratory for Physical Sciences at Microsacle, Hefei, Anhui, China; and Department of Chemistry, The Chinese University of Hong Kong, Shatin, N.T., Hong Kong

Received February 1, 2005; Revised Manuscript Received March 8, 2005

ABSTRACT: Linear poly(*N*-isopropylacrylamide) chains grafted with different contents of short poly(ethylene oxide) branching chains (PNIPAM-*g*-PEO) were prepared by free radical copolymerization of NIPAM and PEO macromonomers (M_w = 5000 g/mol) end-capped with methacrylate in water at 45 °C, higher than the lower critical solution temperature (∼32 °C) of PNIPAM homopolymer. As expected, the copolymerization led to a heterogeneous distribution of PEO on the chain backbone because PNIPAM becomes hydrophobic and fully collapsed at 45 °C. Both the folding and unfolding of individual PNIPAM-*g*-PEO chains in extremely dilute aqueous solutions were investigated by a combination of static and dynamic laser light scattering (LLS). Our results showed that each copolymer chain could indeed fold into a globule without any interchain association when the solution was heated from 25 to 50 °C, resulting in a core−shell nanostructure with a collapsed PNIPAM core and a swollen PEO shell. The folding of the copolymer chains with a higher PEO content involves two transitions; namely, one sharp transition at ∼33 °C and another broader one around ∼45 °C. Such two transitions also occurred in the cooling (unfolding) process. The second transition gradually disappears when we lower the PEO content. A combination of LLS and micro-differential scanning calorimetric results suggests that the first transition is related to the collapse of the PNIPAM segment between two grafted PEO chains. The second one at higher temperatures is related to the steric repulsion-induced stretching and the *n*-clustering-induced collapse of the hydrophilic PEO chains on the periphery of the collapsed PNIPAM core.

Introduction

Protein folding has attracted much attention for a long time and still remains as a challenge and mystery. In general, we can consider protein chains are made of hydrophobic and hydrophilic (charged or none charged) units (amino acid residues). The intra- and interchain hydrogen and/or −S−S− bondings as well as hydrophobic and ionic interaction can lead to some complicated bioactive structures.[1−4] To simplify the problem, polymer researchers tried to prepare amphiphilic copolymer chains made of only one type of hydrophilic monomer and one type of hydrophobic comonomer with different structures either in computation simulation or in real experiments to imitate protein chains.[5,6] Hopefully, the study of the folding of these amphiphilic copolymer chains could shed some light on the complicated problem of the protein folding.

Our previous studies of poly(*N*-isopropylacrylamide) (PNIPAM) homopolymer chains showed that when the temperature is lower than the lower critical solution temperature (LCST ∼ 32 °C), PNIPAM is hydrophilic and exists as individual random coil chains in water, while at higher temperatures, PNIPAM becomes hydrophobic and collapses into individual single-chain globules or stable multichain aggregates (mesoglobules), depending on the solution condition.[7−9] Such an interesting property has made PNIPAM a wonderful model system for the simulation of protein naturation/denaturation in aqueous solution.[1] Shan et al.[10] studied the conformation change of linear PNIPAM chains covalently grafted on the surface of gold nanoparticles by using a highly sensitive microcalorimeter. They showed that the PNIPAM brush can be divided into two zones: the inner zone near the particle surface, in which the chain segments undergo the coil-to-globule transition first and the chain segments in the outer zone collapse only at a higher temperature.

PNIPAM was hydrophobically or hydrophilically modified with different microstructures. In our laboratory, we already modified linear PNIPAM chains by grafting its chain backbone with a very small amount of short PEO chains and studied their folding and association in water.[11,12] There was only one transition for such PEO-modified chains, in which each random coil chain collapses into a core−shell nanostructure with a hydrophobic PNIPAM core and a hydrophilic PEO shell.[11] Later, Zhang et al.[13] modified PNIPAM by evenly inserting short hydrophobic polystyrene segments (20 styrene monomers, called stickers) into its chain backbone and found that such a copolymer chain in water could fold from a random coil to a single flowerlike core−shell nanostructure via an intermediate "ordered coil" conformation. The significance of this study is that it shows that the folding of such a chain involves orientation (flipping) of those hydrophobic stickers before it locks into a final single "flowerlike" nanostructure. It suggests that there might exist orientation of different amino acid residuals of a protein chain prior to its folding (locking in). Tenhu et al.[14,15] studied the influence of the grafted PEO content on the PNIPAM

[†] The Hefei National Laboratory for Physical Sciences at Microsacle.
[‡] University of Science and Technology of China.
[§] The Chinese University of Hong Kong.
* The Hong Kong address should be used for correspondence.

10.1021/ma050222n CCC: $30.25
Published on Web 04/06/2005

Table 1. Characterization of Poly(*N*-isopropylacrylamide)-*g*-PEO Copolymer

samples	PNIPAM-*g*-PEO-48	PNIPAM-*g*-PEO-111	PNIPAM-*g*-PEO-172	PNIPAM-*g*-PEO-316
[NIPAM]/[PEO][a]	48	111	172	316
PEO (wt %)	48	28	20	12
M_w (g/mol)	3.4×10^6	7.2×10^6	9.1×10^6	1.5×10^7
N_{PEO}	321	392	357	326

[a] [NIPAM]/[PEO] refers to number ratio of NIPAM monomers to PEO.

copolymer chain aggregation and found that the chains prepared at different temperatures had different LCSTs and the PEO content has a great effect on the phase transition.

In the present work, we synthesized four PNIPAM-*g*-PEO copolymers with different PEO contents, but a similar chain length, at 45 °C, much higher than its LCST. Our objective is to study the effect of the PEO content on the folding and unfolding of individual amphiphilic copolymer chains in dilute solutions by using a combination of static and dynamic light scattering as well as micro-differential scanning calorimetry. Surprisingly, we found that the copolymer chains with a higher PEO content underwent two transitions. One sharp transition at ~33 °C is related to the collapse of the PNIPAM chain backbone. Another broad transition in the range 35−45 °C disappeared when the PEO content was lower, which can be attributed to the stretching and collapsing of the grafted PEO chains on the periphery.

Experimental Section

Sample Preparation. *N*-Isopropylacrylamide (NIPAM) was purified by recrystallization in a benzene/*n*-hexane mixture. Narrowly distributed poly(ethylene oxide) (PEO) with only one end captured by a hydroxyl group (PEO−OH, M_w = 5000 g/mol, from Fluka) was used as received. Potassium persulfate (KPS) was purified in water. Other chemicals were used without further purification. In the preparation of PEO macromonomers with only one end capped with methacrylate, PEO-OH was first dissolved in anhydrous dichloromethane. Excess amount of methacryloyl chloride was then added dropwise to convert −OH into a methacrylic end group. Triethylamine was added to remove HCl produced. The resultant salt was removed by filtration. The PEO macromonomers were recovered by further purification. The details of the synthesis can be found elsewhere.[16]

The grafting of PEO on poly(*N*-isopropylacrylamide) was done by free radical copolymerization of *N*-isopropylacrylamide with different amounts of PEO macromonomer in water at 45 °C.[12] The reaction was conducted in a 250 mL two-neck flask equipped with a nitrogen inlet tube and a magnetic stirrer. 0.03 mol of NIPAM and different amounts of PEO macromonomer (0.075−0.3 mmol) were added to a proper amount of deionized water to obtain 2 wt % solutions. The KPS/*N,N,N′,N′*-tetramethylethylenediamine (TEMED) redox was used as initiator.[17] The molar ratio of KPS/TEMED is 1:1. The KPS and TEMED were respectively dissolved in water with concentrations of 0.009 and 0.045 M. 5 mL of KPS solution was added into the reaction mixture. The solution was repeatedly degassed at 20 °C and then purged with nitrogen for 0.5 h before the reaction. After the reaction mixture was heated to 45 °C, 1 mL of TEMED solution was added, and the reaction was carried out at this temperature for 45 min in a water bath. The PNIPAM-*g*-PEO copolymers were purified by dialysis in a large amount of water. The final product was dried under a reduced pressure at 40 °C. The copolymer was further purified by several cycles of precipitation/fractionation from an acetone solution to *n*-hexane at 35 °C. Laser light scattering (LLS) and ^{1}H NMR (Bruker DPX-400 spectrometer) was used to characterize each fraction. The ratio of the NMR peak areas of the methylene protons of the *N*-isopropyl group in NIPAM and the methylene protons in PEO was used to estimate the PEO content. The results of four samples used in this study are summarized in Table 1. For LLS study, the solution (4.0×10^{-6} g/mL) was clarified with a 0.45 μm Millipore Millex-LCR filter to remove dust.

Laser Light Scattering. A commercial spectrometer (ALV/DLS/SLS-5022F) equipped with a multitau digital time correlation (ALV5000) and a cylindrical 22 mW Uniphase He−Ne laser (λ_0 = 632 nm) as the light source was used. In static LLS,[18] we can obtain the weight-average molar mass (M_w) and the *z*-average root-mean-square radius of gyration ($\langle R_g^2 \rangle^{1/2}$ or written as $\langle R_g \rangle$) of polymer chains in a dilute solution from the angular dependence of the excess absolute scattering intensity, known as Rayleigh ratio $R_{vv}(q)$, as

$$\frac{KC}{R_{vv}(q)} \approx \frac{1}{M_w}\left(1 + \frac{1}{3}\langle R_g^2 \rangle q^2\right) + 2A_2C \qquad (1)$$

where $K = 4\pi n^2(dn/dC)^2/(N_A\lambda_0^4)$ and $q = (4\pi n/\lambda_0)\sin(\theta/2)$ with N_A, dn/dC, n, and λ_0 being the Avogadro number, the specific refractive index increment, the solvent refractive index, and the wavelength of the laser light in a vacuum, respectively, and A_2 is the second virial coefficient. Strictly speaking, here $R_{vv}(q)$ should be $R_{vu}(q)$ because there is no analyzer before the detector. However, the depolarized scattering of the solution studied is insignificant so that $R_{vu}(q) \sim R_{vv}(q)$. Also, note that in this study the copolymer solution was so dilute that the extrapolation of $C \rightarrow 0$ was not necessary, and the term $2A_2C$ in eq 1 can be dropped.

In dynamic LLS,[19] the Laplace inversion (here the CONTIN method was used) of each measured intensity−intensity time correlation function $G^{(2)}(q,t)$ in the self-beating mode can lead to a line-width distribution $G(\Gamma)$. For a pure diffusive relaxation, Γ is related to the translational diffusion coefficient D by $(\Gamma/q^2)_{C\rightarrow 0, q\rightarrow 0} \rightarrow D$, so that $G(\Gamma)$ can be converted to a transitional diffusion coefficient distribution $G(D)$ or further to a hydrodynamic radius distribution $f(R_h)$ via the Stokes−Einstein equation, $R_h = (k_BT/6\pi\eta)/D$, where k_B, T, and η are the Boltzmann constant, the absolute temperature, and the solvent viscosity, respectively. The simple Cumulant analysis of $G^{(2)}(t)$ of a narrowly distributed sample can effectively lead to an average line width ($\langle\Gamma\rangle$) with a sufficient accuracy.

Micro-Differential Scanning Calorimetry (Micro-DSC). The copolymer solutions were measured by a VP-DSC microcalorimeter (MicroCal Inc) at an external pressure of ~180 kPa. The cell volume was 0.157 mL. The heating rate was 1.0 °C/min, and the instrument response time was set at 5.6 s. All the micro-DSC data were corrected for instrument response time and analyzed using the software in the calorimeter. Note that the copolymer concentration used in DSC was kept at 1.0 mg/mL, much higher than that used in LLS.

Results and Discussion

Figure 1 shows a typical angular dependence of the Rayleigh ratio $[KC/R_{vv}(q)]$ of the copolymer chains in water at three different temperatures: below, near, and above the lower critical solution temperature (LCST ~ 32 °C). On the basis of eq 1, the decrease of the slope with an increasing temperature reflects the decrease of $\langle R_g \rangle$, i.e., the shrinking of the chain. Note that the extrapolation of $KC/R_{vv}(q)$ to $q \rightarrow 0$ at three different temperatures leads to the same intercept, indicating that there was no change in the weight-average molar mass (M_w) during the shrinking process according to eq

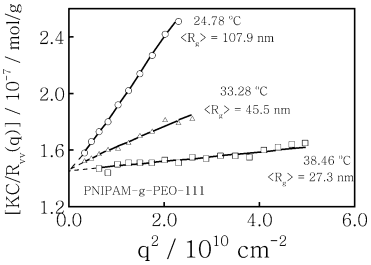

Figure 1. Scattering vector (q) dependence of Rayleigh ratio $R_{vv}(q)$ of copolymer chains in water, where the copolymer concentration is 4.0×10^{-6} g/mL.

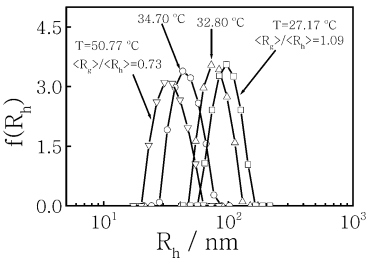

Figure 2. Temperature dependence of hydrodynamic radius distribution $f(R_h)$ of copolymer PNIPAM-*g*-PEO-111 chains in water.

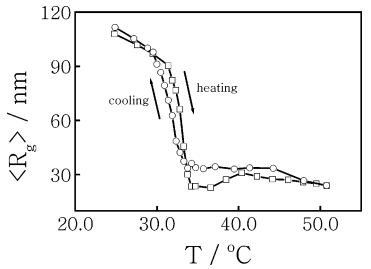

Figure 3. Temperature dependence of z-average root-mean-square radius of gyration ($\langle R_g \rangle$) of copolymer PNIPAM-*g*-PEO-111 chains in water during heating and cooling.

1. In other words, the process indeed involves only individual chains. It should be stated that during the entire heating and cooling cycles the weight-average molar mass M_w of the copolymer PNIPAM-*g*-PEO chains remains a constant within the experimental error (±5%). The scattering intensity was slightly lower around the transition temperature (~33 °C). Previously, we also observed such a small change in the scattering intensity for a PNIPAM homopolymer solution during the chain shrinking but have no clear explanation so far. One possibility would be the dehydration-induced small change of the specific refractive index increment (dn/dc) of the copolymer. The shift of the hydrodynamic radius distribution of the copolymer chains as the temperature increases (Figure 2) directly reveals the coil-to-globule transition of the copolymer chains in water.

Figures 3 and 4 summarize the temperature dependence of $\langle R_g \rangle$ and $\langle R_h \rangle$ of the copolymer chains in water during one cycle of the heating-and-cooling process, where $\langle R_g \rangle$ and $\langle R_h \rangle$ are respectively calculated from each slope in Figure 1 and each distribution in Figure 2. In the heating process, both $\langle R_g \rangle$ and $\langle R_h \rangle$ drop sharply in the range 31−33 °C, reflecting the expected coil-to-globule transition of the PNIPAM chain backbone. Further increase of the temperature first results in slight increases and then followed by slow decreases of both $\langle R_g \rangle$ and $\langle R_h \rangle$ over a broad temperature range. In

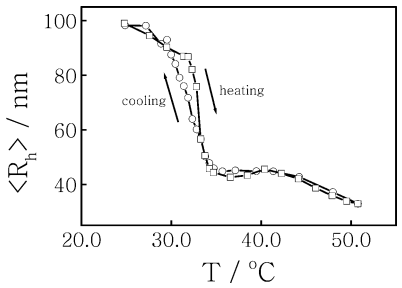

Figure 4. Temperature dependence of average hydrodynamic radius ($\langle R_h \rangle$) of copolymer PNIPAM-*g*-PEO-111 chains in water during heating and cooling.

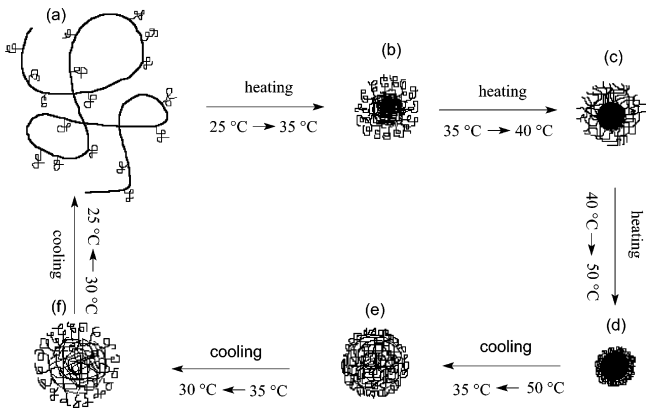

Figure 5. Schematic of the coil-to-globule-to-coil transition of a copolymer PNIPAM-*g*-PEO chain with a higher PEO content during a heating-and-cooling cycle.

comparison with PNIPAM homopolymer chains, such additional changes of both $\langle R_g \rangle$ and $\langle R_h \rangle$ must be related to the grafted PEO chains.

To explain what we have observed in Figures 3 and 4, let us now discuss what has happened during the shrinking of the chain backbone. At lower temperature, each copolymer chain in water exists as a random coil. The heating makes the PNIPAM chain backbone insoluble in water so that it undergoes the coil-to-globule transition. In this process, the hydrophilic PEO chains are forced to stay on the periphery of the globule to form a core−shell nanostructure, such as schematically shown in Figure 5a. The estimated chain density on the PNIPAM core at ~33 °C is ~10 nm^2 per PEO chain. Further shrinking of the PNIPAM core increases the PEO chain density on the surface. As expected, the repulsion between different PEO chains forces them to stretch, as schematically shown in Figure 5b. During this stage, the stretching of the PEO chains in the shell and the collapsing of the PNIPAM chains in the core have opposite effects on the measured $\langle R_g \rangle$ and $\langle R_h \rangle$ when the PEO content is high. The slight increases of both $\langle R_g \rangle$ and $\langle R_h \rangle$ in the range 35−40 °C indicates that here the PEO stretching slightly dominate. As for the slow decreases of both $\langle R_g \rangle$ and $\langle R_h \rangle$ in the high-temperature range (T > 40 °C), there are two possible scenarios as follows.

One is that the shrinking of the PNIPAM core overrides the stretching of the PEO chains in the shell. The other is the n-clustering-induced collapse of the PEO chains because we know that the PEO chains in bulk or in a very concentrated solution have to adopt a random coil conformation.[20,21] In addition, the solvent quality of water for PEO decreases as the solution temperature increases. To differential these two sce-

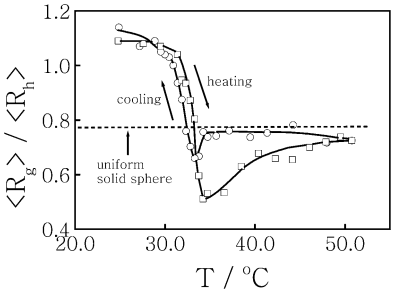

Figure 6. Temperature dependence of ratio of average radius of gyration ($\langle R_g \rangle$) to average hydrodynamic radius ($\langle R_h \rangle$) of copolymer PNIPAM-*g*-PEO-111 chains in water during heating and cooling.

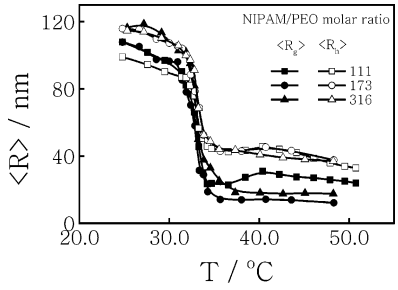

Figure 7. Temperature dependence of *z*-average root-mean-square radius of gyration ($\langle R_g \rangle$) and average hydrodynamic radius ($\langle R_h \rangle$) of copolymer PNIPAM-*g*-PEO chains with different PEO contents in water during heating and cooling.

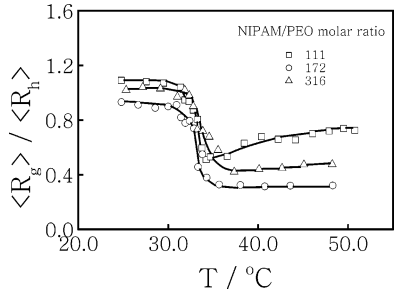

Figure 8. Temperature dependence of ratio of average radius of gyration ($\langle R_g \rangle$) to average hydrodynamic radius ($\langle R_h \rangle$) of copolymer PNIPAM-*g*-PEO chains with different PEO contents in water during heating and cooling.

narios, we plotted the temperature dependence of the ratio $\langle R_g \rangle / \langle R_h \rangle$ (Figure 6) that reflects the chain density distribution. The fact that at lower temperatures $\langle R_g \rangle / \langle R_h \rangle \sim 1.1$, instead of an expected value of ~1.5 for linear chains, can be attributed to the branching structure of the copolymer chains because the PEO chains have a length similar to the PNIPAM segments between two neighboring grafting points. The decrease of $\langle R_g \rangle / \langle R_h \rangle$ from ~1.0 to ~0.5 clearly reveals a change of the chain conformation. It is helpful to note that for a uniform solid sphere, $\langle R_g \rangle / \langle R_h \rangle \sim 0.774$. The lower value of $\langle R_g \rangle / \langle R_h \rangle$ confirms the core−shell structure of the collapsed chain because the collapsed PNIPAM core is denser than the swollen PEO shell.

In comparison with a uniform sphere with the same size, the denser core leads to a smaller $\langle R_g \rangle$, but the same $\langle R_h \rangle$, so that $\langle R_g \rangle / \langle R_h \rangle$ is lower. The increase of $\langle R_g \rangle / \langle R_h \rangle$ in the range 35−40 °C reflects the increase of the shell density because the stretched PEO chains are forced to overlap with each other when the PNIPAM core continues to shrink (Figure 5c). In Figure 6, it is the further increase of $\langle R_g \rangle / \langle R_h \rangle$ in the range 40−50 °C that differentiates the two scenarios. Namely, if the first one was correct, $\langle R_g \rangle / \langle R_h \rangle$ should decrease because the core becomes denser, while in the second scenario, the collapse of the PEO chains increases the chain density of the shell so that the globule becomes more uniform, as schematically shown in Figure 5d. This explains why $\langle R_g \rangle / \langle R_h \rangle$ gradually approaches 0.774.

A combination of Figures 3−5 shows that the reversible globule-to-coil transition does not follow the coil-to-globule path. There exists a hysteresis between the heating and cooling processes. In the cooling process, both $\langle R_g \rangle$ and $\langle R_h \rangle$ have no peak in the range 35−50 °C. The ratio of $\langle R_g \rangle / \langle R_h \rangle$ nearly remains a constant, clearly indicating a uniform swelling, as schematically shown in Figure 5e, very different from the shrinking process. The small dip of $\langle R_g \rangle / \langle R_h \rangle$ at ~33 °C indicates that the collapsed/clustered PEO chains in the shell are finally swollen back to individual coils on the periphery, but the PNIPAM core is still not in the fully swollen state yet, as schematically shown in Figure 5f.

On the other hand, a combination of Figures 7 and 8 reveals that when the PEO content is low, the temperature dependence of $\langle R_g \rangle$, $\langle R_h \rangle$, and $\langle R_g \rangle / \langle R_h \rangle$ has only one transition related to the coil-to-globule transition of the PNIPAM backbone. The transition temperature is close to the LCST (~32 °C) of PNIPAM homopolymer. Moreover, the PEO content has nearly no effect on such a transition. This is expected because when the PEO content is low there is no strong interaction among the PEO chains in the shell. The disappearance of the second transition can also be explained on the basis of the above discussion.

As expected, when the PEO content is not sufficiently high, the grafted PEO chains in the shell are not crowed and pushed together during the coil-to-globule transition of the PNIPAM chain backbone. Figures 7 and 8 indirectly support what we discussed before; namely, the second transition is related to the steric repulsion-induced stretching and then the *n*-clustering-induced collapse of the overlapped PEO chains. A comparison of Figures 3 and 7 reveals that at higher temperatures the copolymer chains with a low PEO content has a smaller $\langle R_g \rangle$ even though they are longer. The difference further reflects the stretching of the PEO chains when the PEO content is higher, as supported by the data in Figure 3. The lower $\langle R_g \rangle / \langle R_h \rangle$ values at higher temperatures in Figure 8 also indicate a lower PEO chain density in the shell.

To further support and justify our discussion about the second transition, we measured the partial heat capacity (C_p) of four PNIPAM-*g*-PEO copolymers with different PEO contents in aqueous solutions using a microcalorimeter. Figure 9 shows that in the heating process the peaks located at ~33 °C are similar, independent of the PEO content. The DSC results agree well with that from LLS. The second broad peak located in the range 40−50 °C gradually disappears at a lower PEO content. It should be noted that in the DSC measurement both the intrachain contraction and the interchain association are involved because a much higher concentration (10^{-3} g/mL) was used in order to have a sufficiently high signal-to-noise ratio. It should be noted that, after investigating both PNIPAM hydrogels and PNIPAM linear chains in water, Laszlo et al.[22] and Ding et al.[23] found two exothermal peaks in the range ~30−33 °C in the cooling process when the scanning rate is very low, but only one endothermic peak in the heating at any heating rate. They attributed

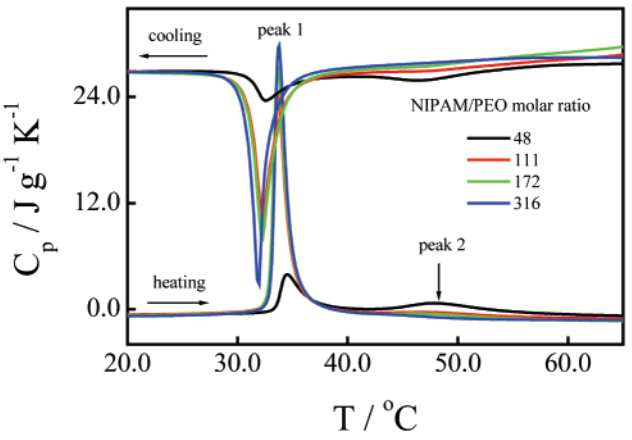

Figure 9. Temperature dependence of partial heat capacity (C_p) of copolymer chains with different PEO contents in water, where the heating rate is 1.0 °C/min.

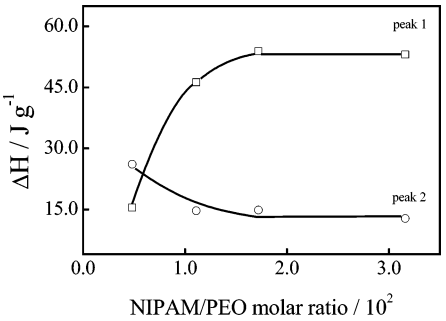

Figure 10. PEO content dependence of endothermic heats for both the transitions in Figure 9.

the additional peak to the kinetic effect. In the current system, the two peaks appear in both the heating and cooling processes and are widely separated and respectively located at ~32 and ~50 °C.

The hysteresis in Figure 9 is obvious around the first transition peak. Such a hysteresis has been attributed to the formation of additional intrachain hydrogen bonding in the collapsed state.[24] The second broad peak reveals that the stretching of the grafted PEO chains and the further collapse of the PNIPAM chains in the core occur over a wider temperature range. Figure 9 further shows that the heating and cooling processes involve a certain amount of endothermic and exothermic heats, respectively. We simply define the area under each peak as a total endothermic or exothermic heat (the change of enthalpy ΔH) for each transition.

Figure 10 shows the PEO content dependence of the change of enthalpy ΔH for both the transitions in Figure 9. For the copolymer chains with a higher PEO content, the average length of the PNIPAM segment between two grafted neighboring PEO chains is short. This is why the peak at ~33 °C related to the PNIPAM segments becomes smaller. On the other hand, when the PEO content decreases, the PNIPAM segments become longer and the PEO shell becomes less crowded so that the peak related to the stretching and collapsing of the grafted PEO chains disappear during the heating process.

Conclusion

The thermally sensitive poly(*N*-isopropylacrylamide)-*graft*-poly(ethylene oxide) (PNIPAM-*g*-PEO) amphiphilic copolymers with different PEO contents can be synthesized by free radical copolymerization of *N*-isopropylacrylamide and PEO macromonomer with an active end at a temperature higher than the lower critical solution temperature (LCST) of the PNIPAM chain backbone. During the polymerization, the PNIPAM chain backbone collapses into a globular form and acts as a template so that the hydrophilic PEO chains are grafted on its surface to form a protein-like heterogeneous distribution of the PEO chains on the PNIPAM chain backbone. The study of the folding and unfolding of such copolymer chains in dilute aqueous solutions by both laser light scattering (LLS) and microcalorimetry reveals that individual copolymer chains can undergo the coil-to-globule-to-coil transition during one heating-and-cooling cycle. At higher temperatures, individual copolymer chains can fold into a core−shell nanostructure with a collapsed PNIPAM core and a swollen PEO shell. When the PEO content is high, there clearly exist two transitions for the folding of the copolymer chains in the heating process. The first sharp transition occurred at ~33 °C is definitely related to the coil-to-globule transition of the PNIPAM chain backbone, which is not influenced by the PEO content. The second transition is over a broad temperature range (35−45 °C), which disappears when the PEO content is low. The change of the ratio of the radius of gyration to the hydrodynamic radius ($\langle R_g \rangle / \langle R_h \rangle$) from a combination of static and dynamic LLS results and the change of enthalpy measured in the micro-DSC suggest that the second transition related to the conformation change of the grafted PEO chains. Presumably, it is related to the repulsion-induced stretching and the *n*-clustering-induced collapsing of the PEO chains in the shell because the PEO chain density on the periphery of the PNIPAM core increases as the PNIPAM core shrinks. Cooling the solution can completely unfold the core−shell single-chain globules, but only one transition was observed, indicating a uniform swelling. There clearly exists a hysteresis between the folding and unfolding processes.

Acknowledgment. The financial support of the National Natural Science Foundation of China (20274045, 50025309, and 90201016) and the Research Grants Council of the Hong Kong Special Administration Region Earmarked Grant 2003/04 (CUHK4029/03P, 2160206) is gratefully acknowledged.

References and Notes

(1) Makhatadze, G. I.; Privalov, P. L. *Adv. Protein Chem.* **1995**, *47*, 307.
(2) Griko, Y. V.; Privalov, P. L. *Biochemistry* **1992**, *31*, 8810.
(3) Nicholson, E. M.; Scholtz, J. M. *Biochemistry* **1996**, *35*, 11369.
(4) Graziano, G. *Int. J. Biol. Macromol.* **2000**, *27*, 89.
(5) Khokhlov, A. R.; Khalatur, P. G. *Phys. Rev. Lett.* **1999**, *82*, 3456.
(6) Timoshenko, E. G.; Kuznetsov, Y. A. *J. Chem. Phys.* **2000**, *112*, 8163.
(7) Wu, C.; Zhou, S. Q. *Macromolecules* **1995**, *28*, 5388.
(8) Wu, C.; Wang, X. H. *Phys. Rev. Lett.* **1998**, *80*, 4092.
(9) Wang, X. H.; Wu, C. *Macromolecules* **1999**, *32*, 4299.
(10) Shan, J.; Chen, J.; Nuopponen, M. Tenhu, H. *Langmuir* **2004**, *20*, 4671.
(11) Wu, C.; Qiu, X. P. *Phys. Rev. Lett.* **1998**, *80*, 620.
(12) Qiu, X. P.; Wu, C. *Macromolecules* **1997**, *30*, 7921.
(13) Zhang, G. Z.; Winnik, F. M.; Wu, C. *Phys. Rev. Lett.* **2003**, *90*, 1.
(14) Virtanen, J.; Baron, C.; Tenhu, H. *Macromolecules* **2000**, *33*, 336.
(15) Virtanen, J.; Tenhu, H. *Macromolecules* **2000**, *33*, 5970.

(16) Wang, P. H.; Pan, C. Y. *J. Appl. Polym. Sci.* **2002**, *86*, 2732.
(17) Siu, M. H.; Zhang, G. Z.; Wu, C. *Macromolecules* **2002**, *35*, 2723.
(18) Chu, B. *Laser Light Scattering*, 2nd ed.; Academic Press: New York, 1991.
(19) Berne, B. J.; Pecora, R. *Dynamic Light Scattering*; Plenum Press: New York, 1976.
(20) Hu, T.; Wu, C. *Macromolecules* **2001**, *34*, 6802.
(21) Hu, T.; Wu, C. *Phys. Rev. Lett.* **1999**, *83*, 4105.
(22) László, K.; Kosik, K.; Geissler, E. *Macromolecules* **2004**, *37*, 10067.
(23) Ding, Y. W.; Ye, X. D.; Zhang, G. Z. *Macromolecules* **2005**, *38*, 904.
(24) Wu, C.; Zhou, S. Q. *Phys. Rev. Lett.* **1996**, *77*, 3053.

MA050222N